Sub-10μm pitch HOT technologies development at Lynred

Laurent Rubaldo, Nicolas Péré-Laperne, Alexandre Brunner, Nicolas Morisset, Christine Laurent Cassillo, Alexandre Kerlain, Cécile Grezes, Gulnar Dagher, Cédric Martin, Clément Lobre, et al.

PROCEEDINGS OF SPIE

SPIEDigitalLibrary.org/conference-proceedings-of-spie

Sub-10µm pitch HOT technologies development at Lynred

Laurent Rubaldo, Nicolas Pere-Laperne, Alexandre Brunner, Nicolas Morisset, Christine Cassillo, et al.

Laurent Rubaldo, Nicolas Pere-Laperne, Alexandre Brunner, Nicolas Morisset, Christine Cassillo, Alexandre Kerlain, Cécile Grezes, Gulnar Dagher, Cedric Martin, Clement Lobre, Olivier Gravrand, Pierre Jenouvrier, David Billon-Lanfrey, "Sub-10µm pitch HOT technologies development at Lynred," Proc. SPIE 12534, Infrared Technology and Applications XLIX, 1253411 (13 June 2023); doi: 10.1117/12.2663462

SPIE.

Event: SPIE Defense + Commercial Sensing, 2023, Orlando, Florida, United States

Sub-10µm pitch HOT Technologies development at LYNRED

Laurent Rubaldo*, Nicolas Pere-Laperne*, Alexandre Brunner*, Nicolas Morisset*, Christine Cassillo*, Alexandre Kerlain*, Cécile Grezes*, Gulnar Dagher**, Cedric Martin*, Clement Lobre***, Olivier Gravrand***, Pierre Jenouvrier* and David Billon-Lanfrey*

*LYNRED, Actipole - CS 10021, 364, route de Valence, 38113 Veurey-Voroize, France
** LYNRED Avenue de la Vauve - CS20018 , 91127 Palaiseau, France
*** CEA-LETI, MINATEC Campus, 17 Rue des Martyrs, 38054 Grenoble Cedex 9, France

ABSTRACT

LYNRED is oriented towards excellence in II-VI, III-V and bolometers technologies, covering all Society's needs in term of infrared detection. Our vision is to preserve and protect, and more than ever, our goal is to provide the right technology to the field missions, spatial and industrial applications, and more generally the right technology to customers' needs. For this purpose we are developing for the next generation pitch, MCT HOT technology, for extended MW band as well as III-V HOT MW blue band technology.

Many challenges have to be addressed for future small pitch, large format and HOT detectors. Electrical and optical crosstalks as well as image quality and stability, are one of the prime concern for detectors with pixel pitch below 10 µm. We will discuss about the trade-off between the different material properties and detector performances to ensure mandatory minimization of Minimum Resolvable Temperature Difference (MRTD) for range optimization.

We will then review latest 7.5µm pitch development at LYNRED, with SXGA formats, based on II-VI and III-V HOT materials, in terms of operability, residual fixed pattern noise (RFPN) and Modulation Transfer Function (MTF) optimizations.

Keywords: III-V, II-VI, HOT, SXGA, 7.5µm pitch, MTF, RFPN, Temporal Noise, RTS.

1. INTRODUCTION

Whatever the application, commercial, spatial or military, the driving forces of products development were:

- Larger format, smaller pitch, consumption and cost reduction
- Improved image quality quantified by the Modulation Transfer Function (MTF) and the couple Residual Fixed Pattern Noise (RFPN)/operability including RFPN (Residual Fixed Pattern Noise) and low frequency noise defects.
- Range increase

To meet the challenges of low SWAPc (Size Weight and Power Cost), LYNRED is developing High Operating Temperature (HOT) II-VI and III-V 7.5µm pitch, in order to respectively address full MW band and blue MW band to cover all applications needs. For tactical applications, like for example Infra-Red Search and Track (IRST) system, the range performance is crucial. In the pitch reduction and HOT contexts, keeping high Modulation Transfert Function (MTF) values is challenging for detector architecture. Moreover we need to keep in mind that not only the MTF has to be optimized but also the Minimum Resolvable Temperature Difference (MRTD). That is to say, we need to optimize MTF while maintaining a high quantum efficiency and the lowest temporal and spatial noise. Following this pass, focal plane arrays with SXGA format have been developed [1] and first promising results have been obtained.

Infrared Technology and Applications XLIX, edited by Gabor F. Fulop, David Z. Ting, Lucy L. Zheng, Proc. of SPIE Vol. 12534, 1253411 · © 2023 SPIE
0277-786X · doi: 10.1117/12.2663462

Based on SXGA 7.5 µm pitch Focal Plane Array (FPA) characterizations, with III-V and p-on-n II-VI technologies and same 14 bits digital ROIC for both FPAs, we will present in section 2 the Quantum Efficiency (QE) measurements. In section 3 we will focus on operability and temporal noise issues. The section 4 will be dedicated to RFPN performances and stability. In section 5 we will focus on MTF measurements and improvements. Before concluding in section 7, section 6 will show some range projections and qualitative comparisons between extended and Blue MW bands.

2. QUANTUM EFFICIENCY MEASUREMENT

2.1 II-VI full MW band SXGA 7.5µm pitch FPA

Quantum Efficiency (QE) is estimated with a Fourier Transform Infrared spectroscope (FTIR) measurement coupled with radiometric measurements to calculate the absolute response in function of the wavelength. Here below is illustrated the normalized and average QE measured with [3.7µm, 4.8µm] filter over 10000 elementary photodiodes. Thanks to radiometric measurements a QE above 75%±5% was estimated.

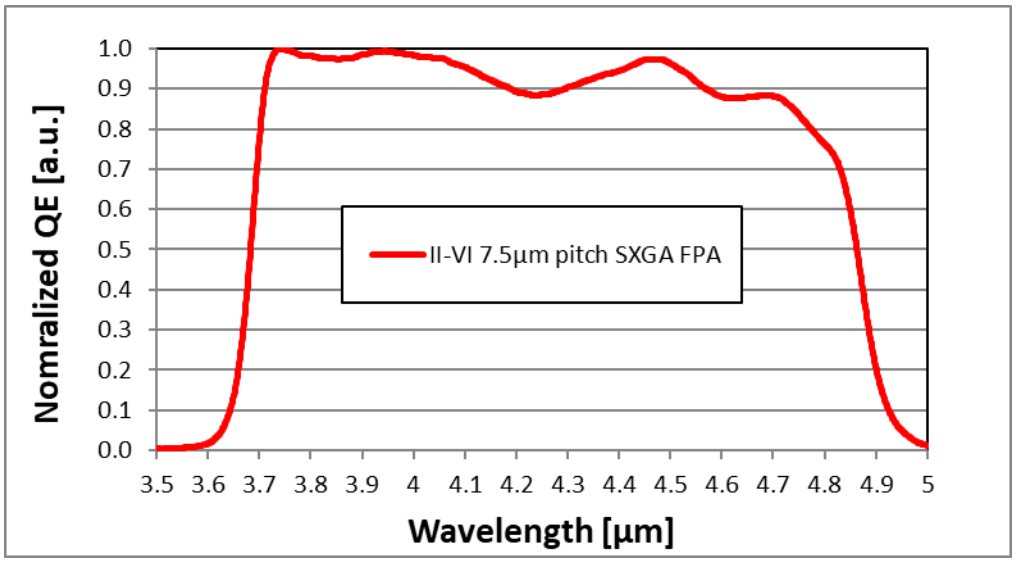

Figure 1 : Normalized QE with [3.7µm, 4.8µm] filter for HgCdTe P/N 7.5µm pitch SXGA format

2.2 III-V blue MW band SXGA 7.5µm pitch FPA

Same approach and method were used for III-V FPA QE measurements. Here below is illustrated the normalized and average QE measured with [3.4µm, 4.2µm] filter over 10000 pixels, a quantum efficiency above 80%±5% was estimated.

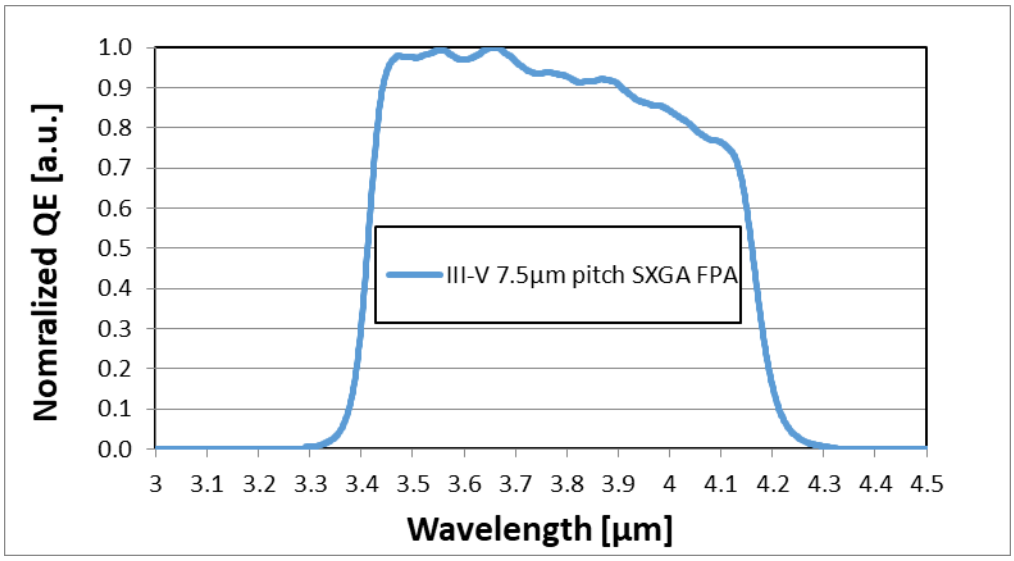

Figure 2 : Normalized QE with [3.4µm, 4.2µm] filter III-V FPA 7.5µm pitch SXGA format

3. TEMPORAL NOISE AND OPERABILITY

3.1 II-VI full MW band SXGA 7.5µm pitch FPA

One of the mandatory figure of merit for image quality to fulfill operational needs is the number of operational pixels and especially noise defects. As illustrated below in logarithmic scale, the well mastered p-on-n HgCdTe technology addressing the full MW band, exhibits quasi-perfect Gaussian temporal noise distribution from 110K to 150K, with almost no tail, except a small one at 150K. The temporal output noise (RMS noise) is measured in front of 20°C black body temperature, with F/3 aperture at 50% Well Fill (WF), over 100 recorded frames.

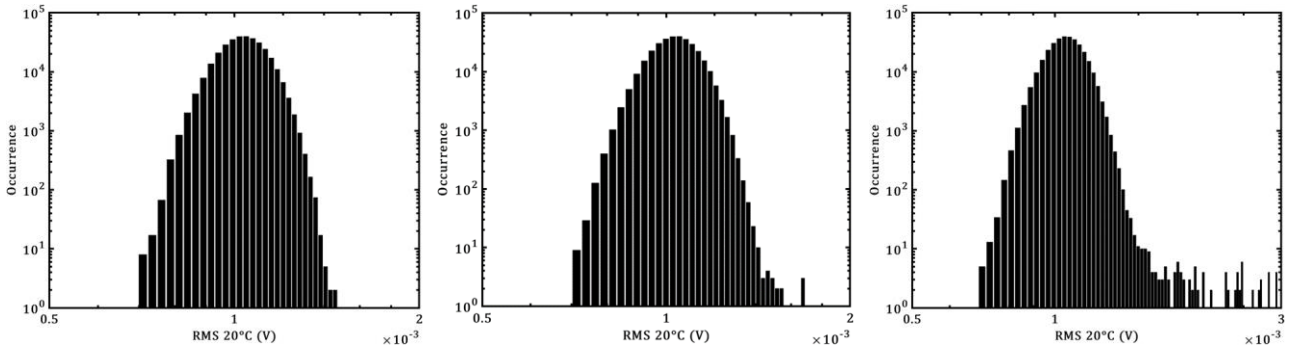

a/ 110K *b/130K* *c/150K*

Figure 3 : Noise histograms at different focal plane temperatures – SXGA Format 7.5µm II-VI technology – F/3 aperture, 50% Well Fill (WF) in front of 20°C black body temperature

An operability above 99.99% at operational temperature of 130K and 99.95% at 150K with a criteria mean RMS ± 100% are obtained.

3.2 III-V blue MW band SXGA 7.5µm pitch FPA

The same quasi-Gaussian shape for RMS noise is obtained for III-V blue MW band technology as illustrated below in logarithmic scale at 150K, F/3 aperture.

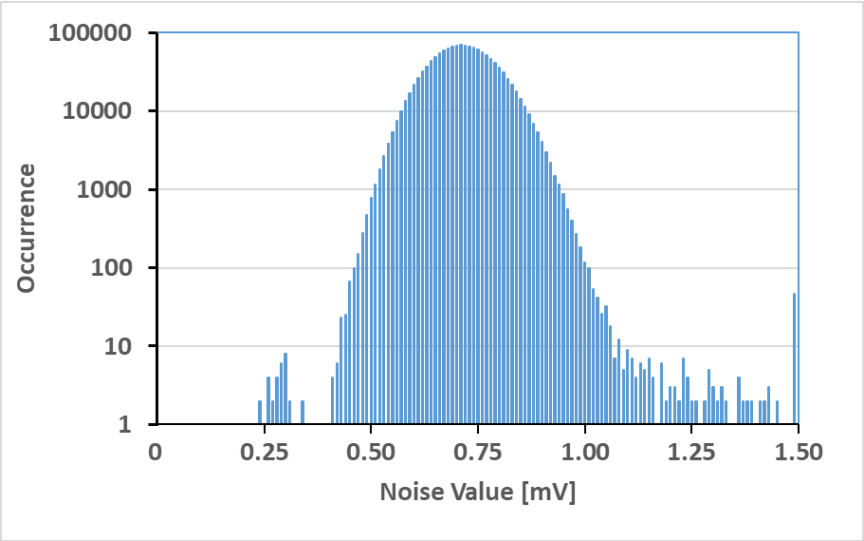

Figure 4 : Noise histograms at 150K – SXGA Format 7.5µm III-V technology – F/3 aperture, 30% WF in front of 15°C black body temperature

Almost no tail is observed, and an operability above 99.99% with a criteria mean RMS ± 100% is obtained at 150K operational temperature with F/3 aperture for this III-V HOT technology addressing

3.3 Random Telegraphic Signal (RTS) studies

RTS [2] defects are a key issue in image calibration and correction. They are at the origin of false alarms and by nature they are difficult to correct. LYNRED has put much effort to quantify properly their main features [3]. Concerning II-VI HOT technology, we found, like previously reported [3], thermal activation of RTS amplitude, up and down state mean times. With temperature increase, RTS amplitudes increase and mean times decrease. This is illustrated below on RTS chronograms obtained at different focal plane temperatures and on Arrhenius plots for amplitude, up and down state mean times for a given RTS defect. Mean times and amplitudes are normalized by values obtained at operational temperature of 130K.

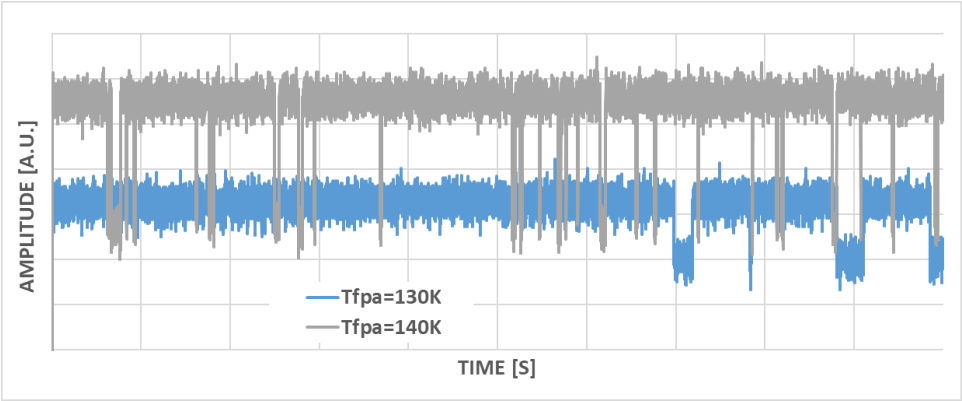

Figure 5 : RTS chronograms at 130K and 140K – SXGA Format 7.5µm II-VI technology – F/3 aperture, 50% WF in front of 20°C black body temperature

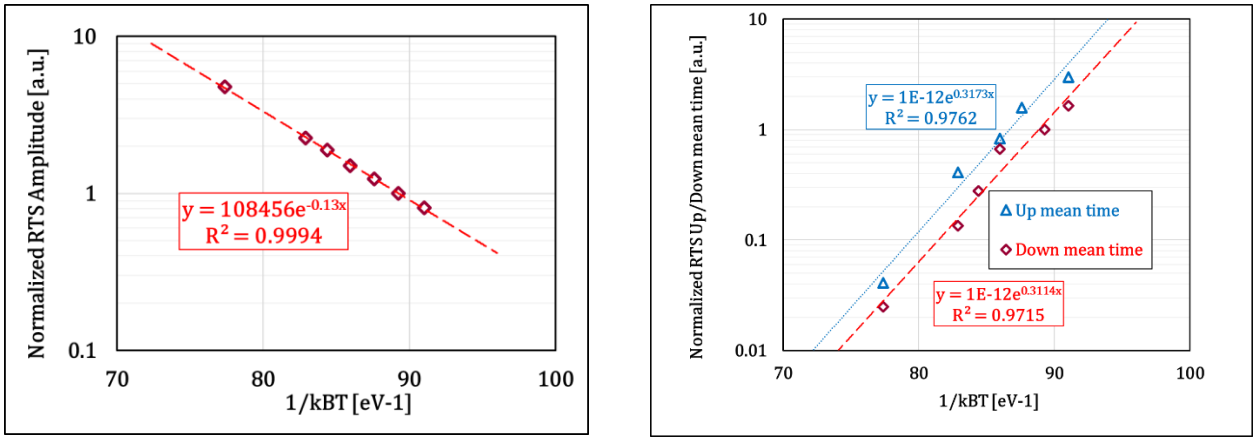

Figure 6 : Normalized Arrhenius plots for RTS amplitudes, up state and down state mean times– SXGA Format 7.5µm II-VI technology – F/3 aperture

For RTS amplitude activation energy, a value close to the mid-gap is obtained, consistent with maximum carrier generation efficiency. For up and down state mean times, activation energies could be seen as emission and capture activation energies from an interrupter defect, based on Hsu model [4]. We have to keep in mind that for carrier emission, activation energy is not an energy level in the bandgap. Based on thermodynamic considerations developed by Van Vechten [5], activation energy is linked to enthalpy variation, and because of entropy factor, activation energy could be greater than the gap. Also an alternative explanation could be given for these activation energies. Up (down) state mean time activation energy could be related to reorientation barrier, from ground up (down) state to ground down (up) state through a saddle point configuration. The barrier is then the energy difference between the saddle point configuration and defect ground states. In this case we obtain barriers very close to each other, highlighting an energy degeneracy of up and down ground states. Further experiments has to be performed to confirm or infirm these statements.

We can also see that the number increase of RTS defects is thermally activated as shown below, with an activation energy, close to RTS amplitude activation energy. Numbers of RTS defects are normalized by value obtained at 130K operational temperature. This suggests that our detection protocol is well set in term of frequency bandwidth, only limited as usual for this kind of parasitic signal, by RTS amplitude.

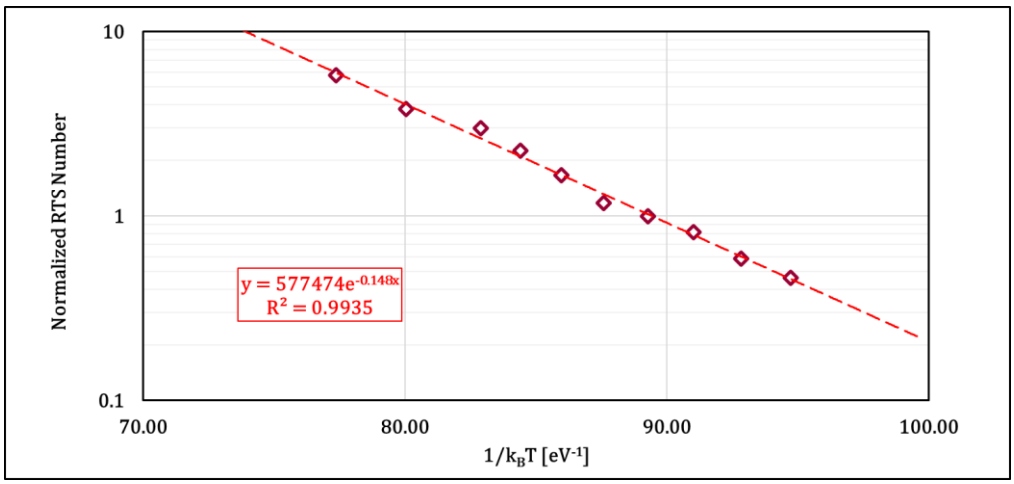

Figure 7 : Normalized Arrhenius plot for RTS amplitudes, up state and down state mean times– SXGA Format 7.5µm II-VI technology – F/3 aperture

Thanks to this precise analysis, a deeper understanding of RTS origins has been built, and then process optimization has been obtained. Consequently, remarkable performances in terms of $1/f^2$ defects have been obtained for II-VI and III-V FPAs, with less than 0.012% RTS defects are observed at respective operational temperature 130K and 150K for SXGA formats.

4. RESIDUAL FIXED PATTERN (RFPN) NOISE AND NON UNIFORMITY CORRECTION (NUC) STABILITY

Thanks to this clear reduction of low frequency noise defects, FPAs exhibit a state of the art RFPN performance. The RFPN is defined as the standard deviation of output signal over all FPA's pixels, after Non-Uniformity Correction (NUC). We will present in the following section the RFPN performances obtained on II-VI and III-V technologies, during the first cool down and after several cool downs over days of experiments performed on IDDCA (Integrated Detector Dewar Cooler Assembly) with F/3 aperture, 7.5µm pitch SXGA formats.

4.1 First cool down

RFPN performances for both technologies are illustrated on the graph below, where the RFPN ratio over temporal noise (RMS noise) is plotted versus well fill. We can see comparable remarkable performances for both technologies, with a ratio RFPN/ RMS noise well below unity in the well fill range [10%, 85%], event below 0.5 in the range [15%, 85%].

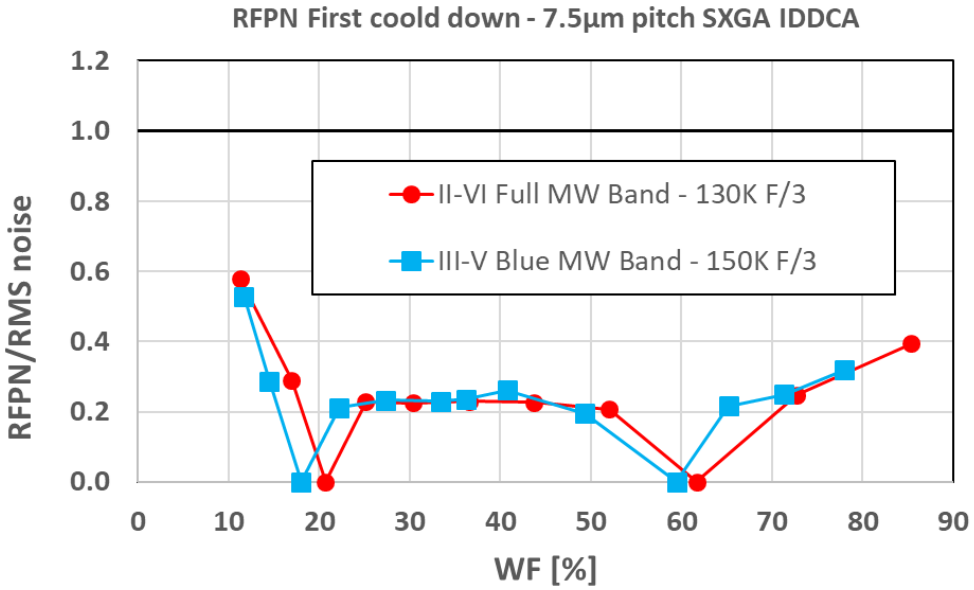

Figure 8: RFPN ratio over RMS noise for III-V and II-VI SXGA format 7.5µm pitch IDDCA F/3 apperture

This high image correctability is completed by a high operability which includes classical criteria ((DC level ± 30%, Responsivity ± 20%, RMS noise ± 100%), RTS defects with a detection protocol defined in [3], and including also RFPN defects defined by the expression below [6]:

$$|NC_{corrected}(x,y) - \overline{NC_{corrected}}| < \overline{NC_{corrected}} \times \alpha \qquad with\ \alpha\ \in [0.3\%, 0.5\%] \qquad (1)$$

where $NC_{corrected}(x,y)$ is the 2-points corrected output level for diode (x,y) and $\overline{NC_{corrected}}$ the mean output corrected level of the FPA

For both technologies, operability including these criteria remain above 99.9%, at 130K for full MW band and 150K for MW blue band, with F/3 aperture.

4.2 RFPN Stability

The stability of NUC correction is mandatory to keep high image quality (low RFPN) over time and cool downs, and range performance. Over several days and multiple cool downs, RFN measurements have been performed using factory NUC (NUC obtained during the first cool dow), with a classical one point refreshment. The two graphs below, illustrate the RFPN performances obtained respectively for II-VI and III-V IDDCA.

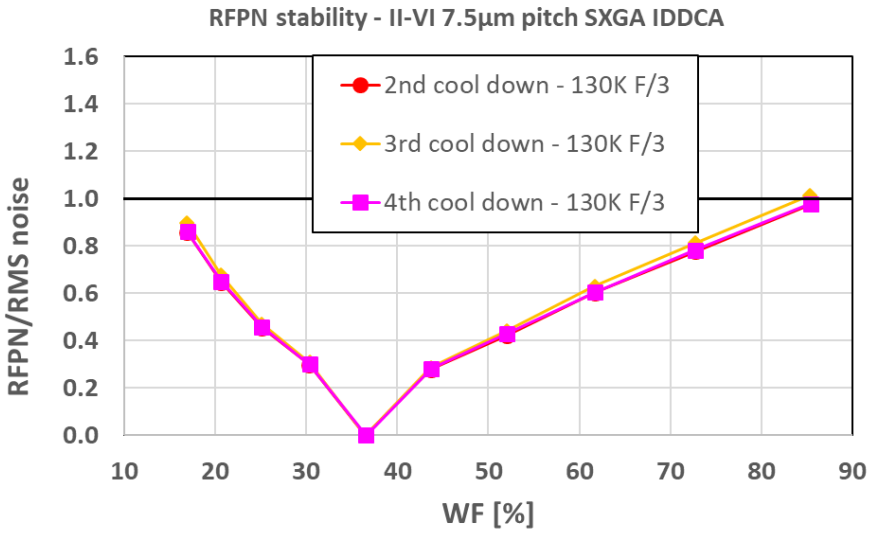

Figure 9 : Stability of RFPN ratio over RMS noise after one point refreshment for II-VI SXGA format 7.5µm pitch IDDCA

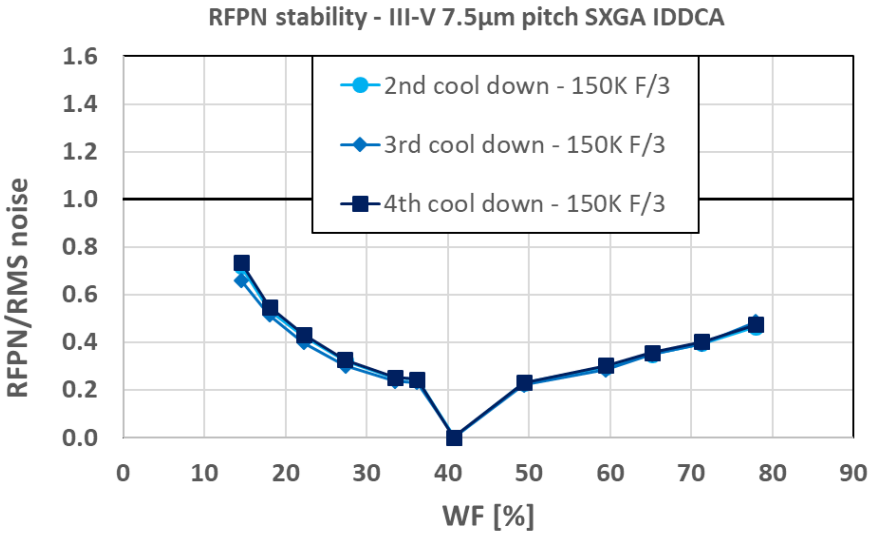

Figure 10 : Stability of RFPN ratio over RMS noise after one point refreshment for III-V SXGA format 7.5µm pitch IDDCA

We can see a better stability for III-V IDDCA. Nevertheless for both technologies, the ratio RFPN over temporal noise remain very stable over several cool downs and below unity.

5. MODULATION TRANSFER FUNCTION (MTF) PERFORMANCES

5.1 Measurements method

MTF is measured with a knife edge method [7]. This technique has been used successfully in the past from 30µm to 10µm [8] pixel pitch. The measured MTF is not directly the pixel MTF due to the optical bench contribution. Aberration and diffraction have to be taken into account, involving a measured MTF degraded by the optical bench.

$$MTF_{measured} = MTF_{pixel} \times MTF_{optical} \quad (2)$$

With this method, it is mandatory to have a good knowledge of the optical MTF. The optical MTF is measured with a specific test photodiode [8] and then simulated with Zernike circle polynomials decomposition [9]. Knowing the optical MTF, pixel MTF can be determined with a deconvolution using the Richardson-Lucy (RL) algorithm [10].

5.2 MTF performances

Following the path used for 10µm pitch II-VI technology [11], consisting in maximising collection volume and minimizing diffusion volume, while maintaining high quantum efficiency and low temporal and spatial noise, outstanding MTF performances have been obtained for II-VI SXGA FPA as illustrated below.

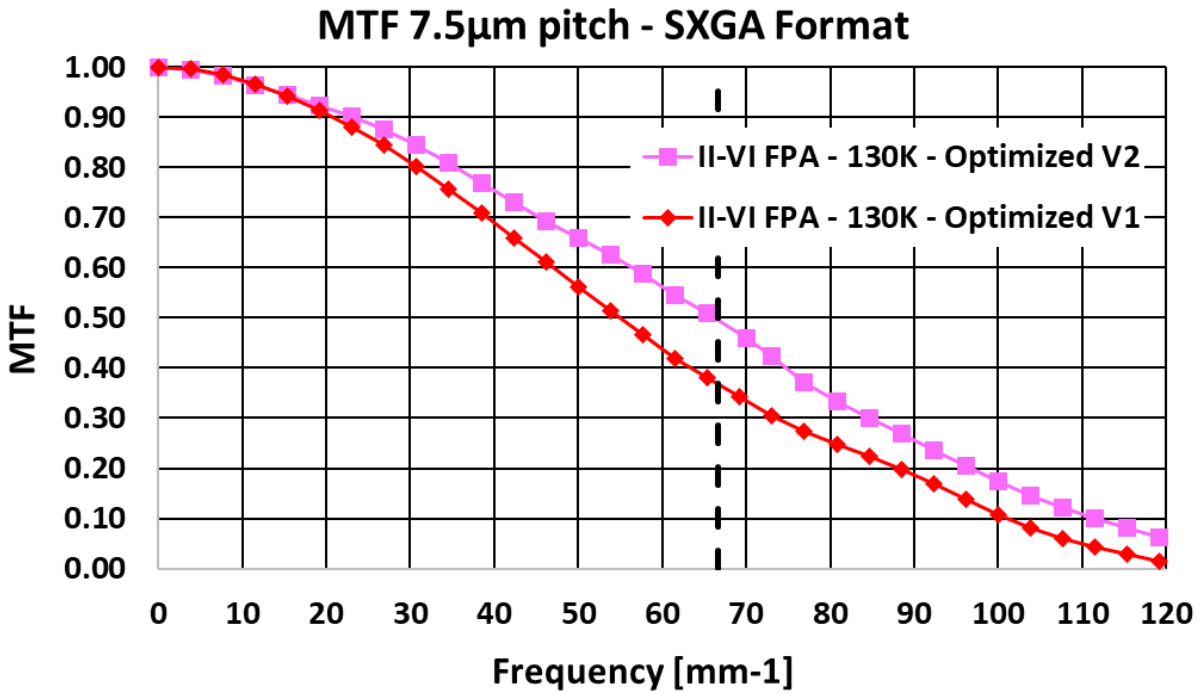

Figure 11: HgCdTe P/N MTF 7.5µm pixel pitch at 130K – SXGA format

In good agreement with previous projections [12], MTF around 0.5 at Nyquist Frequency has been obtained on optimized photodiode design. Same performance is also obtained for III-V FPA.

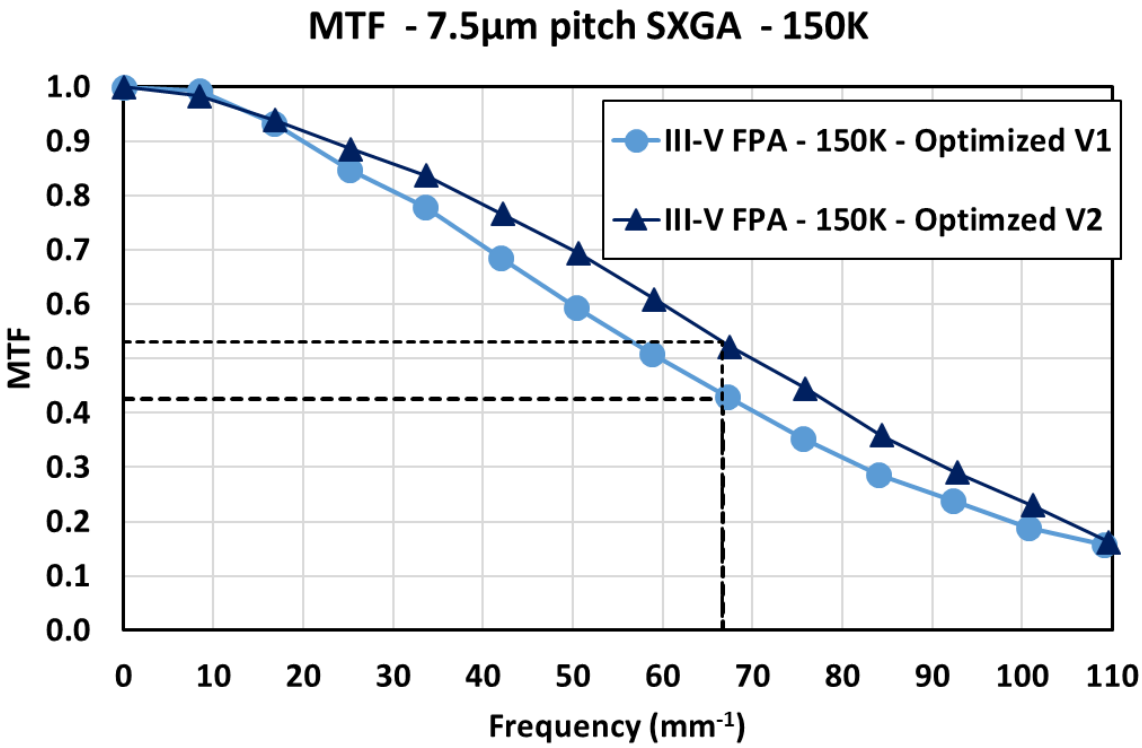

Figure 12: III-V MTF 7.5µm pixel pitch at 150K – SXGA format

6. RANGE EVALUATION

We will detail range estimations for 7.5µm pitch pixels for these two technologies.

6.1 SYSTM OPTIC

The system MTF has many contributors. One of the most important is the optical PSF. Due to diffraction and aberrations, the optical MTF has to be taken into account. In the best case (the diffraction limit), optical MTF depends on the aperture (F#) and the wavelength by the relation:

$$MTF_{optic} = \left|\frac{2}{\pi}\arccos\left(\frac{f}{f_c}\right) - \left(\frac{f}{f_c}\right)\left[1 - \left(\frac{f}{f_c}\right)\right]^{1/2}\right|$$

$$f_c = \frac{1}{F_{\#}\lambda}$$

with f_c the cut-off frequency, F# the aperture and λ the wavelength.

Drigger [13], has shown that a well-sampled case is obtained when:

$$\frac{\lambda F_{\#}}{pitch} = 2$$

In order to fulfil well-sampled criteria, the same optics for both bands was used with F-number $F_{\#} = 3$. The range will be estimated with this value with a focal of 200mm and a circular aperture of 66.66mm.

6.2 SCENE AND RANGE CALCULATION CONDITIONS

The imager conditions are:

- 1280x1024 pixels format.
- An operating temperature of 130K for II-VI FPA and 150K for III-V FPA.
- 1 million electrons well.
- A noise floor of 158 electrons.
- Ratio RFPN/RMS noise equals to 0.5
- Dark currents follow Rule 7 law [14]

The scene conditions are:

- A temperature difference target-background of 2K.
- Two background temperatures: -20°C , 40°C
- An object of 2.3x2.3x5.6 m^3.
- Two different atmosphere absorptions : one Mid-latitude atmosphere and one Tropical atmosphere, with 5 km visibility, simulated with MODTRAN 5.

Classical Johnson criteria have been used: for the detection, a 1 line pair with the probability of 50% is chosen. For the identification 6 lines pair with the same probability is taken.

6.3 RANGE COMPARISONS

The tables below summarizes the range evaluations with tropical atmosphere, at 50% WF with background temperature of 40°C for III-V and II-VI technologies.

	III-V IDDCA – 150K	II-VI IDDCA – 130K
Detection - 40°C [km]	20.2	16.6
Identification - 40°C [km]	4.3	3.7

Table I : Range estimation in km for III-V and II-VI IDDCA – Tropical atmosphere visibility 5 km

We obtained for both technologies, identification ranges in the order of 4 km. We can see, as expected because of lower atmosphere absorption and diffraction issue, a better range for the blue MW band, around 17% higher identification range and almost 22% higher detection range.

Ranges have also been evaluated on mid-latitude atmosphere under low flux condition with -20°C background temperature, with a fixed integration time of 20 ms.

	III-V IDDCA – 150K	II-VI IDDCA – 130K
Detection - 20°C [km]	15.8	16.2
Identification- 20°C [km]	3.9	3.7

Table II : Range estimation in km for III-V and II-VI IDDCA – Mid-latitude atmosphere low flux condition visibility 5 km

Because of NETD and frame frequency issues in low flux conditions, blue MW band and extended MW band exhibit very similar ranges, within few percent differences in our simulation conditions with F/3 aperture, 20ms integration time. This highlights the complementarity of both technologies to cover a wide set of operational needs.

7. CONCLUSION

To meet the challenges of low SWAPc (Size Weight and Power Cost), High Operating Temperature (HOT) II-VI and III-V 7.5µm pitch technologies are under development at LYNRED. SXGA FPA with same digital ROIC have been designed to address full MW band and blue MW band. We summarized the latest exhaustive electro-optical characterizations in terms of QE, spatio-temporal noise and MTF. For both technology, remarkable performances have been shown with QE ranging from 75% to 80%, operability above 99.9% including RTS and RFPN defects. Very low and stable RFPN has been demonstrated. While keeping very low spatio-temporal noise and high QE, for range issues, outstanding MTF performances have been achieved, with a value around 0.5 at Nyquist frequency for III-V and II-VI 7.5µm pitch SXGA FPA. Some ranges projections have been detailed, with higher ranges obtained with blue MW band, but also comparable ones for full MW band in low flux conditions. Besides the spectral needs for extended MW band (lower sunlight flux, higher plume irradiance) this underlines the complementarity between the two bands. LYNRED, thanks to its III-V and II-VI SXGA 7.5µm picth with a same ROIC interface and their excellent performances, can cover exhaustively and in a versatile way applications and costumers needs in the MW band.

8. ACKNOWLEDGMENTS

The authors would like to thank all the Lynred and LETI/CEA (LIR) teams, dedicated to quality work and to challenging wins, as well as the French MoD for their support of these work.

9. REFERENCES

[1] O. Gravrand, C. Lobre, J.L. Santailler, N. Baier; W. Rabaud; A. Kerlain, D. Sam-Giao, P. Leboterf, B. Cornus and L. Rubaldo, Proceedings SPIE 12107, Infrared Technology and Applications XLVIII, (2022).

[2] S. Machlup, J. Appl. Phys. Vol. 25, pp. 341-343 (1954).

[3] A. Brunner, L. Rubaldo, V. Destefanis, F. Chabuel, A. Kerlain, D. Bauza, and N. Baier, ” Improvement of RTS Noise in HgCdTe MWIR Detectors,” Journal of Electronic Material, Vol. 43 no. 8, p. 3060-3064 (2014).

[3] A. Brunner, L. Rubaldo, V. Destefanis, F. Chabuel, A. Kerlain, D. Bauza, and N. Baier, ” Improvement of RTS Noise in HgCdTe MWIR Detectors,” Journal of Electronic Material, Vol. 43 no. 8, p. 3060-3064 (2014).

[4] S. Hsu, J. Whittier et C. Mead, «Physical model for burst noise in semiconductor devices,» Solid State Electron., vol. 13, n°17, pp. 1055-1071, 1970.

[5] J. Van Vechten et C. Thurmond, «Entropy of ionization and temperature variation of ionization levels of defects in semiconductors,» Phys. Rev. B, vol. 14, n°18, pp. 3539-3550, 1976.

[6] L. Rubaldo, P. Guinedor, A. Brunner, V. Destefanis, P. Fougères, A. Kapferer, D. Sam-giao, L. Dargent, A. Kerlain, A. Cathignol, V. Compain, F. Boulard, D. Brellier and O. Gravrand, “Achievement of high image quality MCT sensors with Sofradir vertical industrial model”, Proc. Infrared Technology and Applications XLIV, vol. 10614, (2018)

[7] I. A. Cunningham et A. Fenster, « A method for modulation transfer function determination from edge profiles with correction for finite-element differentiation », Med. Phys., vol. 14, no 4, p. 533-537, juill. 1987.

[8] J. Berthoz., R. Grille, L. Rubaldo, O. Gravrand, A. Kerlain, N. Pere-laperne, L. Martineau, F. Chabuel, and D. Leclercq « Modeling and characterization of MTF and spectral response at small pitch on Mercury Cadmium Telluride », J. Electron. Mater., vol. 44, no 9, p. 3157-3162, 2015.

[9] J. D. Schmidt, « Numerical simulation of optical wave propagation with examples in MATLAB », 2010.

[10] W. H. Richardson, « Bayesian-based iterative method of image restoration », JoSA, vol. 62, no 1, p. 55-59, 1972.

[11] N. Péré-Laperne, L.Rubaldo, A. Kerlain, E. Carrère, L. Dargent, R. Taalat and J. Berthoz "10µm pitch design of HgCdTe diode array in Sofradir"», Proc. SPIE Quantum Sensing and Nanophotonic Devices XII, 9370, 2015.

[12] J.Berthoz, L; Rubaldo, A; Brunner, M. Maillard, G. Vojetta, N. Jomard, S. Courtas, N. Péré-Laperne, F. Rochette, Olivier Gravrand, znd D. Billon-Lanfrey, « Range infrared detector issues in the SWAPc and pitch reduction context, », Proc. Infrared Technology and Applications XLVi, vol. 1140715, (2020).

[13] R. G. Driggers, R. H. Vollmerhausen, J. P. Reynolds, J. D. Fanning, et G. C. Holst, « Infrared detector size: how low should you go? », Opt. Eng., vol. 51, no 6, p. 063202, 2012.

[14] W. E. Tennant, « “Rule 07” revisited: Still a good heuristic predictor of p/n HgCdTe photodiode performance? », J. Electron. Mater., vol. 39, no 7, p. 1030-1035, 2010.